Dynamic Stabilization of a Quantum Many-Body Spin System

T. M. Hoang, C. S. Gerving, B. J. Land, M. Anquez, C. D. Hamley, and M. S. Chapman*

School of Physics, Georgia Institute of Technology, Atlanta, Georgia 30332-0430, USA

We demonstrate dynamic stabilization of a strongly interacting quantum spin system realized in a spin-1 atomic Bose-Einstein condensate. The spinor Bose-Einstein condensate is initialized to an unstable fixed point of the spin-nematic phase space, where subsequent free evolution gives rise to squeezing and quantum spin mixing. To stabilize the system, periodic microwave pulses are applied that rotate the spin-nematic many-body fluctuations and limit their growth. The stability diagram for the range of pulse periods and phase shifts that stabilize the dynamics is measured and compares well with a stability analysis.

Recent advances in ultracold atomic physics provide opportunities to investigate unstable equilibrium phenomena of interacting quantum many-body systems featuring well-characterized and controllable Hamiltonians [1]. By changing the dimensionality of the system, tuning the interaction strength [2], or magnetically quenching a spin system [3,4], it is possible to study excitations across quantum phase transitions and apparent relaxation to non-thermal steady states [5]. Beyond these fundamental investigations, nonequilibrium dynamics can be used to generate squeezed states [6–10] and non-Gaussian states [11] that are potential resources for quantum enhanced measurements [12] and quantum information processing [13].

It is well known that unstable equilibria of physical systems can be dynamically stabilized by external periodic forcing. The inverted pendulum stabilized by vibrating the pivot point (Kapitza's pendulum) provides a classic example of this nonintuitive phenomenon and was first demonstrated over 100 years ago [14]. Dynamical stabilization has a broad range of applications including rf ion traps, mass spectrometers [15], and particle synchrotrons [16]. Dynamic stabilization of nonequilibrium many-body Bose-Einstein condensates has been suggested by tuning the sign of the scalar [17–20] and spin-dependent [21] interaction strength and by time varying the trapping potential in a double-well Bose-Einstein condensate [22–24]. Related ideas have been employed to suppress tunneling in optical lattice systems as a means to control the superfluid-Mott insulator phase transition [25].

In this Letter we demonstrate dynamic stabilization of a strongly interacting quantum many-body spin system by periodic manipulation of the phase of the states. The experiment employs a spin-1 atomic Bose condensate initialized to an unstable (hyperbolic) fixed point of the phase space, where subsequent free evolution gives rise to spin-nematic squeezing [6,26] and quantum spin mixing [11,27,28]. To stabilize the system, periodic microwave pulses are applied that manipulate the spin-nematic quantum correlations and coherently limit their growth.

The range of pulse periods and phase shifts with which the condensate can be stabilized is measured and compares well with a linear stability analysis of the problem. The experiment is conceptually related to spin decoupling or refocusing techniques used in NMR [29] and bang-bang control of noninteracting two-level quantum systems (qubits) in quantum information processing [30]. The novelty of this work is the application of these concepts to the collective dynamics of an interacting quantum spin system.

The experiment uses a small spin-1 rubidium-87 condensate satisfying the single mode approximation such that it contains just a single domain. The dynamical evolution then occurs only in the internal spin degrees of freedom, which simplifies the many-body problem to a zero-dimensional system (a microcondensate [31]) of interacting quantum spins. This permits a description using macroscopic quantum variables such as the collective spin operators [26,27], $\hat{S}_i$ ($i \in x, y, z$), in terms of which the many-body Hamiltonian can be written [6]

$$\hat{\mathcal{H}} = \lambda \hat{S}^2 + \frac{q}{2} \hat{Q}_{zz}, \tag{1}$$

where λ is the spinor interaction energy integrated over the condensate, $\hat{S}^2 = \hat{S}_x^2 + \hat{S}_y^2 + \hat{S}_z^2$ is the total spin operator, $q \propto B^2$ is the quadratic Zeeman energy, $\hat{Q}_{zz} = (2/3)\hat{N}_1 + (2/3)\hat{N}_{-1} - (4/3)\hat{N}_0$ is an element of the spin-1 nematic (quadrupole) tensor, and $\hat{N}_k = \hat{a}_k^\dagger \hat{a}_k$, ($k = 0, \pm1$) is the number operator for each of the spin projections of the condensate. The Hamiltonian conserves the total number of atoms $\hat{N} = \hat{N}_1 + \hat{N}_{-1} + \hat{N}_0$ and the magnetization $\hat{S}_z = \hat{N}_1 - \hat{N}_{-1}$, and exhibits a quantum phase transition at $q = -4N\lambda$ for $\lambda < 0$, as is the case here.

For $S_z = 0$, the condensate has an unstable equilibrium point at $N_0 = N$ for small quadratic Zeeman energies; in the neighborhood of this point, the linearized equations of motion in the rotating frame are given by

$$\dot{\hat{S}}_x = -q\hat{Q}_{yz}, \qquad \dot{\hat{Q}}_{yz} = (4N\lambda + q)\hat{S}_x, \tag{2}$$

with identical equations for $(\hat{S}_y, \hat{Q}_{xz})$ reflecting the rotational symmetry about the z axis (see the Supplemental Material [32]). These equations describe a quantum (many-body) inverted harmonic oscillator that is inherently unstable. The nature of the instability is illustrated with the aid of the mean-field spin-nematic phase space represented on a unit sphere with axes $\{S_\perp, Q_\perp, x\}$, where $S_\perp^2 = S_x^2 + S_y^2$, $Q_\perp^2 = Q_{xz}^2 + Q_{yz}^2$, and $x = 2N_0/N - 1$ (see the Supplemental Material [32]) [6,33]. This sphere is shown in Fig. 1 together with the mean-field dynamical orbits of the system for $q < 4N|\lambda|$. The unstable fixed point is located at the intersection of the two manifolds of a separatrix that divides the space into phase-winding and oscillatory phase orbits. The mean-field phase space is functionally identical to the symmetric double-well Bose-Hubbard model [34,35], and both can be described using a classical nonrigid pendulum [36,37] where the unstable fixed point corresponds to an inverted pendulum.

The experiment begins with a condensate containing $N = 4.5 \times 10^4$ atoms with trap frequencies of $\omega \approx 2\pi \times 250$ Hz that is initialized in the $|f = 1, m_f = 0\rangle$ hyperfine state held in a high magnetic field (2 G). To initiate spin dynamics, the condensate is rapidly quenched below the quantum critical point by lowering the magnetic field to 220 mG. This is a nonevolving state in the mean-field limit; however, the exact quantum solution [27] shows evolution that generates Gaussian squeezed states at early times [6] and a rich variety of non-Gaussian states at later times that eventually destabilize the system and lead to evolution away from the fixed point [11]. In our experiment, dynamic

stabilization is achieved by preventing the buildup of these correlations using periodic phase shifts of the spinor wave function that manifest as a rotation about the polar axis of the spin-nematic phase space illustrated in Fig. 1. The rotation is implemented using 2π Rabi pulses on the $|f = 1, m_f = 0\rangle \leftrightarrow |f = 2, m_f = 0\rangle$ microwave clock transition that effectively shift the phase of the $|f = 1, m_f = 0\rangle$ spinor component by an amount $\Delta\theta_0 = \pi(1 + \Delta/\sqrt{1 + \Delta^2})$, where $\Delta = \delta/\Omega$ is the detuning normalized to the on-resonance Rabi rate [6]. Long-term stabilization is realized by periodic repetition of the sequence shown in Fig. 1. Although the technique is illustrated using a rotation angle corresponding to the angles between the manifolds of the separatrix, the condensate can be stabilized for a range of rotation angles, as shown below.

The experimental results demonstrating dynamic stabilization of the condensate are shown in Fig. 2. The time evolution of the spin population $\rho_0 = N_0/N$ is shown for different microwave pulse parameters chosen to produce a stabilized condition (case A), a marginally unstable condition (case B), and a more unstable condition (case C). The unstabilized dynamics showing free evolution spin mixing is shown for comparison. In the stabilized cases, the pulse period is 60 ms with the first pulse at 32 ms after the quench. The difference between cases A, B, and C is
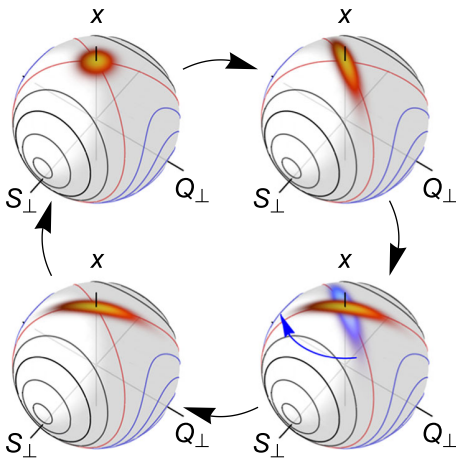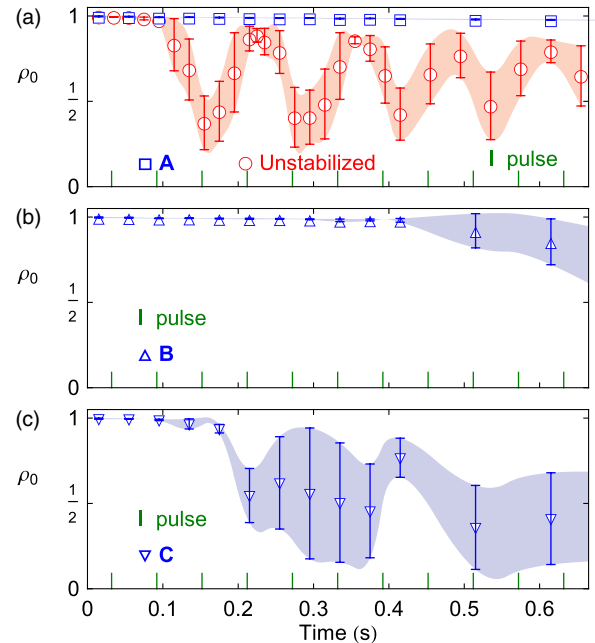

FIG. 1 (color online).   Illustration of the experimental concept. The condensate is initialized at the pole of the spin-nematic sphere with Heisenberg-limited uncertainties in $S_\perp$ and $Q_\perp$ (upper left). Initial evolution produces squeezing along the diverging manifold of the separatrix (upper right). The quantum state is quickly rotated [gray (blue) arrow] to the converging manifold of the separatrix using a microwave field pulse (lower right). Subsequent evolution of the rotated state (lower left) unsqueezes the condensate, returning it close to the original state (upper left).

FIG. 2 (color online).   Evolution of ρ_0 measured for different applied phase shifts (blue squares, up or down triangles), compared with the unstabilized case (red circles). (a) Case A, $\Delta\theta = -0.65\pi$, is well stabilized, (b) case B, $\Delta\theta = -0.724\pi$, is at the margin of stability, and (c) case C, $\Delta\theta = -0.56\pi$, is unstable. The pulse period is 60 ms for all cases, and the pulse times are indicated as green ticks. The region encompassed by the shading is a second order interpolation of the standard deviation to guide the eye.

the size of quadrature phase shift applied per pulse. Each measurement is repeated 10–15 times and the mean and standard deviation are shown with the marker and error bar.

We have investigated the range of pulse periods and quadrature phase shifts that provide stabilization of the spin dynamics. These measurements are shown in Fig. 3, which displays a map of the stability region versus pulse period and quadrature phase shift (modulo π, the periodicity of the phase space). The stability criterion applied is $\bar{\rho}_0 > 0.85$ for 3 runs at 185 ms of evolution indicated by the dark gray (green) region corresponding to maximum dip in unstabilized case. The locations corresponding to the time sequences (cases A–D) are indicated on the stability map. The data are compared with a linear stability analysis of Eq. (2) (see the Supplemental Material [32]). The stability condition from this analysis is shown as the solid red lines in Fig. 3 for a spinor dynamical energy $c \equiv 2N\lambda = -2\pi\hbar \times 7.2(2)$ Hz (measured using coherent spin oscillations) and the measured magnetic field $B = 220(10)$ mG that determines the quadratic Zeeman effect $q = 2\pi\hbar \times 71.6 \times B^2$ Hz/G^2. The data are in good overall agreement with the theory: for shorter pulse periods, the condensate is stabilized with a wide range of quadrature phase shifts, while for long pulse periods, the range of quadrature phase shifts capable of stabilizing the dynamics shrinks and reaches an asymptotic value close to the angle between branches of the separatrix, $\Delta\theta = \cos^{-1}(-1 - q/c)$. The green region extends slightly beyond the linear stability
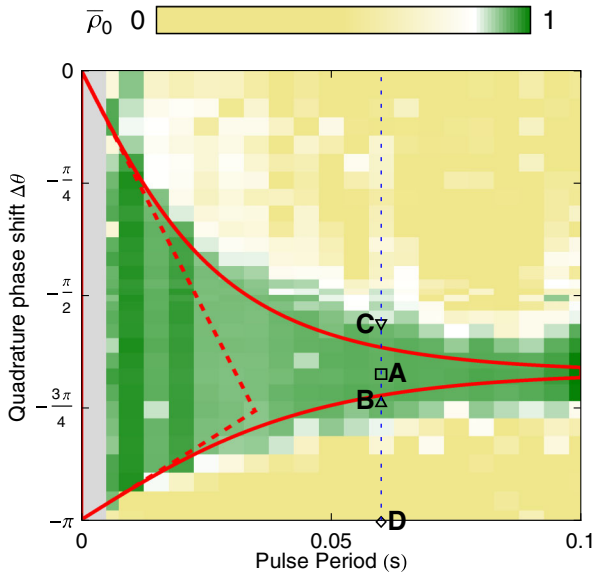
analysis because, for the marginally unstable cases, the dynamics have not had enough time to "fall off" the top of the sphere in 185 ms.

Compared to previous proposals for stabilizing dynamics in the double-well system [22] or the spin-1 condensate [21] based on periodic reversals of the *sign* of q (or λ), our method is based on periodically changing the *magnitude* of q. The effect of the periodic microwave pulses can be approximated by a time-averaged Hamiltonian with an effective quadratic Zeeman energy, $q_{\text{eff}} = q + \hbar\Delta\theta/\tau$. It is an interesting question, however, whether or not our observed stability is explained solely by this effect. For both $q_{\text{eff}} > 4N|\lambda|$ and $q_{\text{eff}} < 0$ there is no longer a hyperbolic fixed point centered on the pure $m_f = 0$ state but rather an elliptical fixed point, and hence, wherever these conditions are met, the time-averaged system will be inherently stable. This defines a "robust" stability region that is shown as dashed red lines in Fig. 3. Although this region agrees asymptotically with the linear stability analysis (solid red lines) for shorter pulse periods, the robust region is much smaller. All of the measurements presented are outside of the robust region except for the determination of the stability map. This demonstrates that the time-averaged Hamiltonian is insufficient to describe the results.

We have performed two additional measurements to demonstrate that stabilizing pulses maintain the quantum features of the spin dynamics. In the first, we have studied the evolution of the condensate under periodic pulses with $\Delta\theta = -\pi$ (case D), which should have no effect on the dynamics. The results, shown in Fig. 4(a), verify that the condensate undergoes normal quantum spin mixing on the same time scale as without stabilization pulses [11]. In the second measurement, shown in Fig. 4(b), we turn off the stabilization pulses after 572 ms and show that
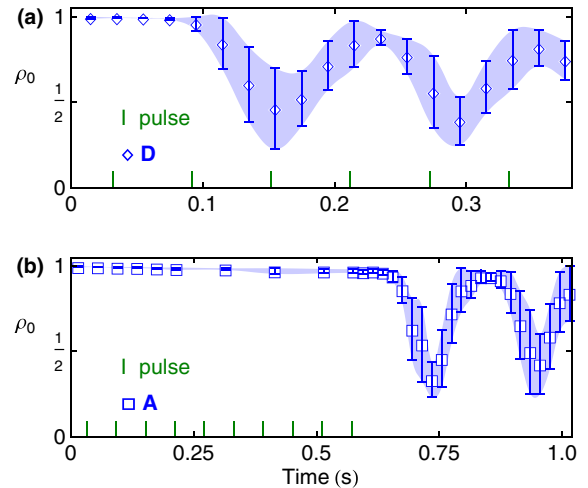

FIG. 3 (color online).   Map of the measured stability region for ρ_0 population after 185 ms of evolution. Stable regions are shaded dark gray (green) and unstable regions are shaded light gray (yellow) while the analytic stability solution is indicated by a solid red line. Also shown is the "robust" region determined from a time-averaged effective Hamiltonian (red dashed line). The markers A–D indicate the pulse parameters used for the data in the other figures.

FIG. 4 (color online).   (a) Evolution of ρ_0 for $\Delta\theta = -\pi$ (case D in Fig. 3). (b) Evolution of ρ_0 for 572 ms of stabilization with $\Delta\theta = -0.65\pi$ (case A) followed by free evolution. The region encompassed by the shading is a second order interpolation of the standard deviation to guide the eye.
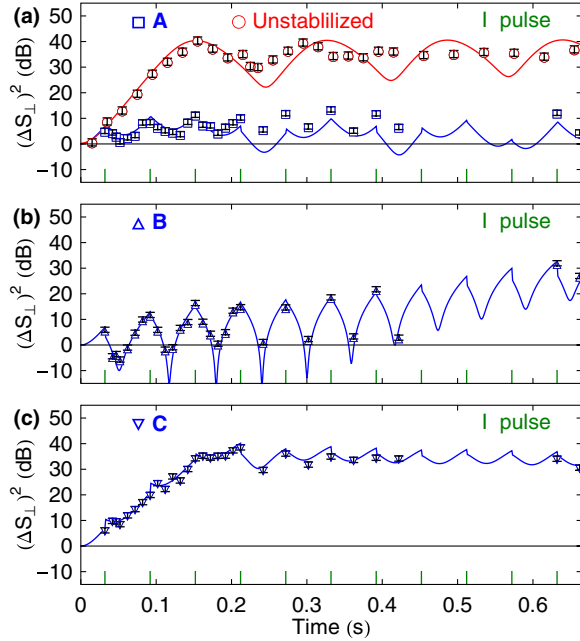
FIG. 5 (color online). Evolution of the variance of the transverse magnetization $(\Delta S_\perp)^2$ measured for different applied phase shifts (blue squares, up and down triangles) compared with the unstabilized case (red circles). Pulse parameters are the same as for Fig. 2. Solid lines are quantum simulations using Eq. (1).

the system again undergoes normal spin mixing. The fact that these two experiments demonstrate spin mixing on the same time scale as the unstabilized case is important in that spin mixing from the $m_f = 0$ state is sensitive to excess noise in the initial states [11,28]. Extra noise is particularly noticeable in the duration of the initial pause (or "break time") in the dynamics of ρ_0, where any added noise decreases its length. Even after more than half a second of stabilization, this pause is still 100 ms in length.

Measurement of the spin population $\rho_0 = N_0/N$ corresponds to a measurement of the projection of the spin-nematic sphere on the polar axis. Hence, this metric is admittedly less sensitive to early dynamics of the state initialized at the pole and does not directly reveal the growth and control of the quantum fluctuations of the initial state discussed in the introduction. To access this physics more directly, we have measured the evolution of the fluctuations of the transverse magnetization $(\Delta S_\perp)^2$ by performing a rf rotation prior to measurement of the spin populations [6]. These measurements are shown in Fig. 5 for the same stabilization pulse parameters as above. Each measurement is repeated 30 times in order to accurately determine the variance. These results are compared with a fully quantum calculation based on Eq. (1) where the initial state is a Fock state with 4.5×10^4 atoms in $m_f = 0$ and the atom loss is accounted for by time varying the spinor dynamical rate (see the Supplemental Material [32]). For the unstabilized condensate, the fluctuations

grow exponentially by a factor of 10^4 within 150 ms and eventually execute small oscillations near the maximum value. When the condensate is stabilized, the fluctuations of $S_\perp$ exhibit periodic growth and reduction during each pulse cycle, which reflect the squeezing and unsqueezing of the condensate. In the short time scale up to 0.4 s, the data are in good agreement with the quantum calculation. The stabilized data (case A) show the expected periodic evolution of the fluctuations and also show a dramatic reduction of the fluctuations compared with the unstabilized condensate. The measurements of the fluctuations do not fall below the standard quantum limit because the principle axes of the squeezing ellipse (shown schematically in Fig. 1 for this case) are never oriented along the measurement basis. For case B, the "nonideal" quadrature phase rotation and intervening evolution periodically align the minor axis of the squeezing ellipse to the $S_\perp$ axis such that the fluctuations go below the standard quantum limit indicated by the 0 dB line, while in case C the fluctuations grow similarly to the unstabilized case.

The experiments presented above demonstrate dynamical stabilization of the spin dynamics of a spin-1 condensate. This is a many-body effect in that the spin dynamics of the condensate are driven by coherent collisional interactions in a Bose condensate. The experiments reveal genuine quantum dynamics beyond the mean field as demonstrated by the preservation of quantum spin mixing shown in Fig. 4 and the control of the quantum fluctuations $(\Delta S_\perp)^2$ shown in Fig. 5. We stress, however, that the stabilization technique is applicable for states with classical noise or quantum noise. Hence, the claim for "quantum" control of the dynamics (beyond the trivial point that the condensate is an inherently quantum entity) rests on the fact that the measured quantum fluctuations and characteristic features of quantum spin mixing are preserved by the method. Although the stabilization is demonstrated with a microcondensate for which the spatial dynamics are factored out, these methods should be applicable to the control of the coupled spin or spatial dynamics that lead to domain formation in larger condensates. In future investigations, it would be interesting to explore this area as well as the application of these concepts to finite temperature spin systems.

*mchapman@gatech.edu
[1] I. Bloch, J. Dalibard, and W. Zwerger, Rev. Mod. Phys. **80**, 885 (2008).
[2] C. Chin, R. Grimm, P. Julienne, and E. Tiesinga, Rev. Mod. Phys. **82**, 1225 (2010).

[3] L. E. Sadler, J. M. Higbie, S. R. Leslie, M. Vengalattore, and D. M. Stamper-Kurn, Nature (London) **443**, 312 (2006).

[4] D. M. Stamper-Kurn and M. Ueda, Rev. Mod. Phys. **85**, 1191 (2013).

[5] A. Polkovnikov, K. Sengupta, A. Silva, and M. Vengalattore, Rev. Mod. Phys. **83**, 863 (2011).

[6] C. D. Hamley, C. Gerving, T. Hoang, E. M. Bookjans, and M. S. Chapman, Nat. Phys. **8**, 305 (2012).

[7] C. Gross, T. Zibold, E. Nicklas, J. Estève, and M. K. Oberthaler, Nature (London) **464**, 1165 (2010).

[8] M. F. Riedel, P. Böhi, Y. Li, T. W. Hänsch, A. Sinatra, and P. Treutlein, Nature (London) **464**, 1170 (2010).

[9] C. Gross, H. Strobel, E. Nicklas, T. Zibold, N. Bar-Gill, G. Kurizki, and M. K. Oberthaler, Nature (London) **480**, 219 (2011).

[10] B. Lücke, M. Scherer, J. Kruse, L. Pezz, F. Deuretzbacher, P. Hyllus, O. Topic, J. Peise, W. Ertmer, J. Arlt et al., Science **334**, 773 (2011).

[11] C. Gerving, T. Hoang, B. Land, M. Anquez, C. Hamley, and M. Chapman, Nat. Commun. **3**, 1169 (2012).

[12] J. Ma, X. Wang, C. Sun, and F. Nori, Phys. Rep. **509**, 89 (2011).

[13] S. L. Braunstein and P. van Loock, Rev. Mod. Phys. **77**, 513 (2005).

[14] A. Stephenson, Philos. Mag. **15**, 233 (1908).

[15] W. Paul, Rev. Mod. Phys. **62**, 531 (1990).

[16] E. D. Courant, M. S. Livingston, and H. S. Snyder, Phys. Rev. **88**, 1190 (1952).

[17] H. Saito and M. Ueda, Phys. Rev. Lett. **90**, 040403 (2003).

[18] H. Saito, R. G. Hulet, and M. Ueda, Phys. Rev. A **76**, 053619 (2007).

[19] R. L. Compton, Y.-J. Lin, K. Jiménez-García, J. V. Porto, and I. B. Spielman, Phys. Rev. A **86**, 063601 (2012).

[20] F. K. Abdullaev, J. G. Caputo, R. A. Kraenkel, and B. A. Malomed, Phys. Rev. A **67**, 013605 (2003).

[21] W. Zhang, B. Sun, M. S. Chapman, and L. You, Phys. Rev. A **81**, 033602 (2010).

[22] N. Bar-Gill, G. Kurizki, M. Oberthaler, and N. Davidson, Phys. Rev. A **80**, 053613 (2009).

[23] E. Boukobza, M. G. Moore, D. Cohen, and A. Vardi, Phys. Rev. Lett. **104**, 240402 (2010).

[24] F. Sols and S. Kohler, Laser Phys. **14**, 1259 (2004).

[25] A. Zenesini, H. Lignier, D. Ciampini, O. Morsch, and E. Arimondo, Phys. Rev. Lett. **102**, 100403 (2009).

[26] L.-M. Duan, J. I. Cirac, and P. Zoller, Phys. Rev. A **65**, 033619 (2002).

[27] C. K. Law, H. Pu, and N. P. Bigelow, Phys. Rev. Lett. **81**, 5257 (1998).

[28] C. Klempt, O. Topic, G. Gebreyesus, M. Scherer, T. Henninger, P. Hyllus, W. Ertmer, L. Santos, and J. J. Arlt, Phys. Rev. Lett. **104**, 195303 (2010).

[29] R. Ernst, G. Bodenhausen, and A. Wokaun, Principles of Nuclear Magnetic Resonance in One and Two Dimensions (Clarendon Press, Oxford, 1987).

[30] L. Viola and S. Lloyd, Phys. Rev. A **58**, 2733 (1998).

[31] A. Lamacraft, Phys. Rev. A **83**, 033605 (2011).

[32] See Supplemental Material at http://link.aps.org/supplemental/10.1103/PhysRevLett.111.090403 for derivation of the analytic stability region. Additionally, we provide details of the $\{S_\perp, Q_\perp, x\}$ phase space representation and the quantum simulation used to compare the experimental results to theory.

[33] L. I. Plimak, C. Weiß, R. Walser, and W. P. Schleich, Opt. Commun. **264**, 311 (2006).

[34] A. Vardi and J. R. Anglin, Phys. Rev. Lett. **86**, 568 (2001).

[35] E. Kierig, U. Schnorrberger, A. Schietinger, J. Tomkovic, and M. K. Oberthaler, Phys. Rev. Lett. **100**, 190405 (2008).

[36] A. Smerzi, S. Fantoni, S. Giovanazzi, and S. R. Shenoy, Phys. Rev. Lett. **79**, 4950 (1997).

[37] W. Zhang, D. L. Zhou, M.-S. Chang, M. S. Chapman, and L. You, Phys. Rev. A **72**, 013602 (2005).